

Multi-band Superconductivity in the Chevrel Phases SnMo_6S_8 and PbMo_6S_8

A.P. Petrović¹, R. Lortz², G. Santi¹, C. Berthod¹, C. Dubois¹, M. Decroux¹, A. Demuer³,
A.B. Antunes³, A. Paré³, D. Salloum⁴, P. Gougeon⁴, M. Potel⁴, and Ø. Fischer¹

¹*DPMC-MaNEP, Université de Genève,
Quai Ernest-Ansermet 24, 1211 Genève 4, Switzerland*

²*Department of Physics,
The Hong Kong University of Science & Technology,
Clear Water Bay, Kowloon, Hong Kong*

³*Laboratoire des Champs Magnétiques Intenses CNRS,
25 rue des Martyrs, B.P. 166,
38042 Grenoble cedex 9, France*

⁴*Sciences Chimiques, CSM UMR CNRS 6226,
Université de Rennes 1, Avenue du Général Leclerc,
35042 Rennes Cedex, France*

(Dated: November 22, 2021)

Sub-Kelvin scanning tunnelling spectroscopy in the Chevrel Phases SnMo_6S_8 and PbMo_6S_8 reveals two distinct superconducting gaps with $\Delta_1 = 3$ meV, $\Delta_2 \sim 1.0$ meV and $\Delta_1 = 3.1$ meV, $\Delta_2 \sim 1.4$ meV respectively. The gap distribution is strongly anisotropic, with Δ_2 predominantly seen when scanning across unit-cell steps on the (001) sample surface. The spectra are well-fitted by an anisotropic two-band BCS *s*-wave gap function. Our spectroscopic data are confirmed by electronic heat capacity measurements which also provide evidence for a twin-gap scenario.

PACS numbers:

Among the vast zoo of poorly-understood superconductors, Chevrel Phases (CP) stand out for their high upper critical fields H_{c2} , many of which exceed the Pauli limit [1]. These materials were first synthesised in 1971 [2] and enjoyed a wealth of attention in the early 1980s. Unfortunately, the discovery of the cuprate superconductors largely swept CP under the laboratory carpet, despite a lack of detailed understanding of their large H_{c2} values. A multi-band scenario (incorporating strong-coupling effects and enhanced spin-orbit scattering) was suggested as a possible explanation [3], but until now this hypothesis has remained experimentally unexplored.

Multi-band superconductivity was first proposed 50 years ago as a potential avenue for increasing critical temperatures [4]. Interband scattering between non-degenerate bands at the Fermi level E_F enables superconductivity to be induced in bands which may not directly participate in the pairing mechanism, thus increasing the effective density of states (DoS) and hence the transition temperature T_c . However, with the exception of some transition metal calorimetric data [5] and tunnelling in doped SrTiO_3 [6], multi-band superconductivity remained a largely theoretical concept until the discovery of MgB_2 in 2001 revived interest in the field [7]. In this material, superconductivity in the quasi-2D σ -band induces coherence in the quasi-3D π -band with an unexpectedly high T_c of 39 K. The two gaps have been imaged by a variety of techniques, including local spectroscopic [8] and bulk thermodynamic approaches [9]. Recently, evidence has been found for multi-band superconductivity in borocarbides [10], sesquicarbides [11], skutterudites [12] and,

perhaps most interestingly, pnictides [13]. CP and pnictides share similar anomalously large values of H_{c2} and do not follow standard Werthamer-Helfand-Hohenberg theory. However, in contrast with the pnictides, the Mo_6X_8 ($X = \text{S}, \text{Se}$) Chevrel cluster does not exhibit any intrinsic magnetism or competing order. This greatly simplifies the analysis and interpretation of its low-temperature properties, particularly any multi-band effects. Band-structure calculations have indicated the presence of two Mo *d* bands at E_F in CP [14]: in this Letter we present local spectroscopic evidence for two distinct superconducting gaps in SnMo_6S_8 and PbMo_6S_8 . These data are supported by specific heat measurements displaying clear signatures of a second gap.

We have chosen to focus on SnMo_6S_8 and PbMo_6S_8 since these two materials have the highest values for T_c and H_{c2} within the CP family: 14.2 K, ~ 40 T and 14.9 K, > 80 T respectively [15]. Single crystals of each compound with typical volume 1 mm^3 were grown at 1600°C by a chemical flux transport method using sealed molybdenum crucibles. Their high purity was confirmed by AC susceptibility (ACS) yielding $\Delta T_c = 0.1$ K for SnMo_6S_8 and 0.3 K for PbMo_6S_8 . Local spectroscopy (STS) was performed on room-temperature-cleaved samples with a home-built helium-3 scanning tunnelling microscope in high-vacuum ($< 10^{-7}$ mbar), using a lock-in amplifier technique. Heat capacity measurements were carried out at the Grenoble High Magnetic Field Laboratory with a high-resolution microcalorimeter using the “long relaxation” technique [16] and in Geneva using a Quantum DesignTM PPMS.

The first hint of a two-band order parameter arises from fast spectroscopic traces over several tens of nanometers in the (001) plane of each material (Fig. 1). The corresponding topography in SnMo_6S_8 shows atomically flat terraces separated by steps of size $12 \pm 1 \text{ \AA}$, which compares favourably with twice the rhombohedral unit cell parameter 6.5 \AA . Spectra taken on the terraces are homogeneous, with a gap of 2.95 meV and a marked lack of any quasiparticle excitations within the gap. In contrast, spectra taken on the steps between terraces display additional peaks at lower energy, suggestive of a second gap. We interpret this as a local modification of the tunnelling matrix element, enabling us to preferentially probe another portion of the Fermi surface with different atomic orbital characters. Cleaved surfaces of PbMo_6S_8 are of rather lower quality with an RMS roughness of $\sim 1.5 \text{ \AA}$ and broad poorly-resolved unit cell-sized steps (Fig. 1(b)(iii)). However, the average spectrum (Fig. 1(b)(ii)) displays a kink at $\sim \pm 1.4 \text{ meV}$ (highlighted by arrows) and a V-shaped dispersion around E_F . This confirms the presence of states within the large gap.

Such a dramatic spectral variation as a function of the local topography has not previously been observed in any other superconductor. It may therefore be natural to suggest that the isolated appearance of these multi-gap signatures at unit cell steps could be due to a surface bound state or defect. However, a localised state would not display the particle-hole symmetry of the peaks we observe. We have imaged a large number of separate unit cell steps and a second gap is consistently observed upon scanning across them. Another explanation for the double-gap behaviour could be the proximity effect inducing weak superconductivity in a metallic surface layer [17]. However, the small gap induced would vary strongly with the thickness of the surface metallic layer. Apart from the fact that measurements are performed on freshly-cleaved samples, thus rendering any surface layer deposition implausible, a layer of metallic impurities would not be expected to have a uniform thickness. This would cause substantial variation in the size of the induced gap and an extremely high zero-bias conductance (ZBC), both of which are incompatible with our data.

In Figure 2 we display a range of spectra with fits using a multi-band model. The Bardeen-Cooper-Schrieffer (BCS) quasiparticle density of states for an anisotropic s -wave n -band superconductor may be written as

$$N(\omega) = \sum_{j=1}^n \frac{N_j}{2\pi} \int_0^\pi \text{Re} \left[\frac{(\omega + i\Gamma_j)\text{sign}(\omega)d\theta}{\sqrt{(\omega + i\Gamma_j)^2 - \Delta_j^2 F_j^2(\theta)}} \right] \quad (1)$$

where N_j is the contribution of band j to the DoS at E_F , Γ_j the scattering rate due to lifetime effects, Δ_j the magnitude of the gap within band j and $F_j(\theta) = a_j + (1 - a_j) \cos \theta$ measures the anisotropy of the corresponding gap with $0.5 < a_j < 1$. We include the temperature and the experimental smearing (0.3 meV) before

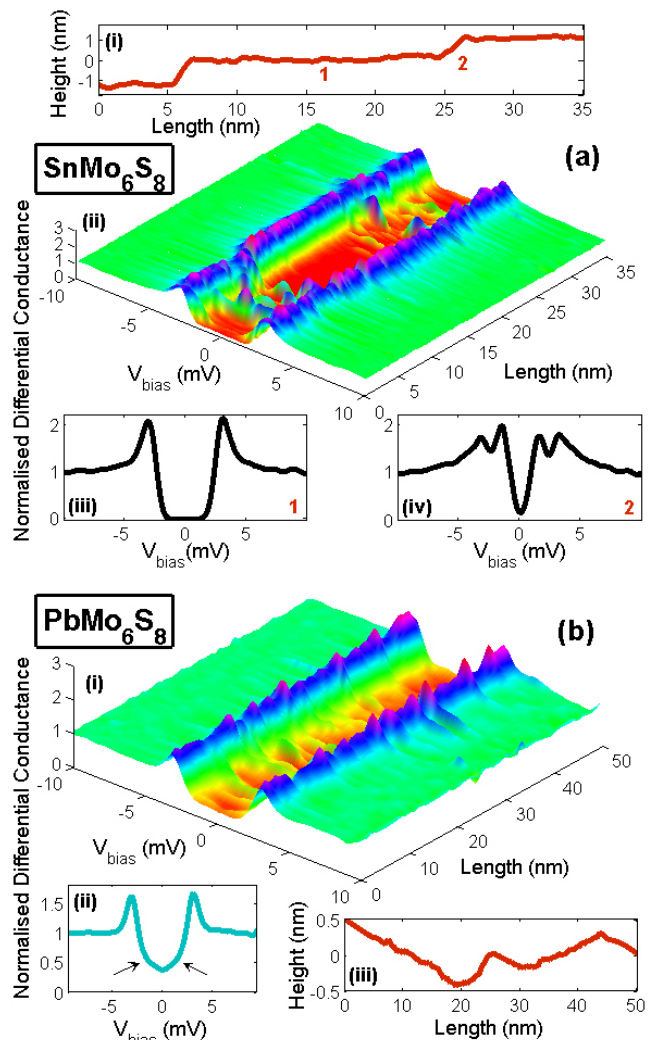


FIG. 1: (a) Zero-field 35nm trace on SnMo_6S_8 taken at $T = 0.4\text{K}$, junction resistance $R_T = 0.03 \text{ G}\Omega$. (i) Topography showing double unit-cell steps; (ii) spectroscopic trace; (iii,iv) individual spectra taken on a flat terrace (1) and above a unit-cell step (2). (b) Zero-field 40nm trace on PbMo_6S_8 taken at $T = 0.5\text{K}$, $R_T = 0.015 \text{ G}\Omega$. (i) Spectroscopic trace; (ii) average spectrum from entire trace; (iii) topographic variation. All data are raw and unaveraged.

performing least-squares fits to our data with N_j , Δ_j , F_j and Γ_j as free parameters. Note that the spectral backgrounds between $\pm 5\text{-}10 \text{ meV}$ are rather poorly-fitted, which is indicative of strong coupling to a low-energy phonon. However, a full Eliashberg analysis of the spectra is beyond the scope of this Letter.

Atomically flat surfaces in SnMo_6S_8 produce homogeneous spectra (Fig 2(a)) which may be fitted using only a single band (i.e. $n=1$ in (1)). There is a slight deterioration in the fit quality at low energy, which is attributed to a very small contribution from the second band. In contrast, Fig. 2(b) shows the average of around 50 spectra acquired above a unit cell step. There is clearly a

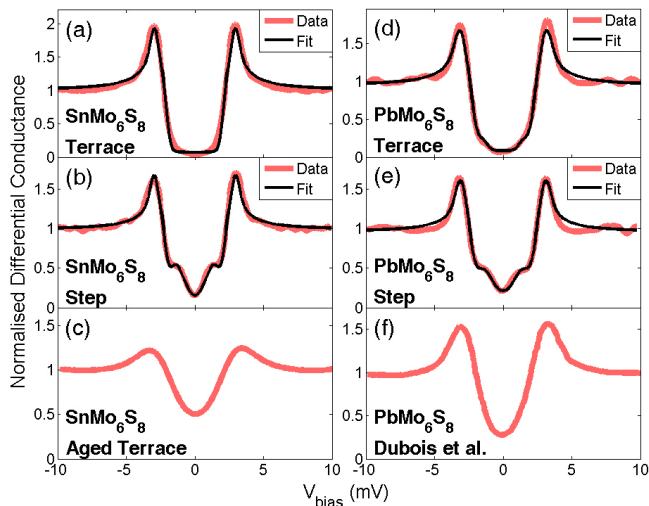


FIG. 2: (a-c) SnMo_6S_8 spectra and fits taken at 0.4 K, $R_T = 0.03 \text{ G}\Omega$. (d-e) PbMo_6S_8 spectra and fits taken at 0.5 K, $R_T = 0.015 \text{ G}\Omega$. (f) PbMo_6S_8 spectrum taken at 1.9 K, $R_T = 0.025 \text{ G}\Omega$ from [18]. See text for details and table I for fit parameters.

significant contribution from the smaller gap, necessitating a two-band fit. Similar fits are carried out on spectra from a flat zone and a broad step in PbMo_6S_8 and the parameters obtained listed in Table I. We find $2\Delta_1/k_B T_c \sim 5$ in each compound, but Δ_2 is 30-40 % larger in PbMo_6S_8 than SnMo_6S_8 . In both materials the gap anisotropies are similar: a small anisotropy in H_{c2} ($\epsilon^2 = 0.67$) has been observed in PbMo_6S_8 [3], but with the present data we are unable to judge whether this is due to the anisotropy in Δ_1 or Δ_2 . We believe it unwise to draw quantitative conclusions on the symmetry of Δ_2 , since our experiment has a finite resolution imposed by a 0.3 meV broadening from the lock-in. However, any interband scattering will preclude a pure d -wave order parameter in Δ_2 due to the dominant isotropic s -wave component in Δ_1 .

Previous STS experiments on PbMo_6S_8 provided evidence for low-energy excitations within the superconducting gap, but lacked sufficient resolution to distinguish two separate gaps. This is due to three factors: sample age, temperature and environment. In [18], measurements were performed on old crystals at 1.9 K in an exchange gas, compared with freshly-grown samples at 0.4-0.5 K and high vacuum in the present work. The increased thermal broadening at 1.9 K blurs the two gaps, though this should not be sufficient to render the smaller gap invisible. The major factor here is a deterioration in the sample surface due to the exchange gas environment. It is well-known that in a two-band superconductor, interband scattering due to impurities mixes the two gaps and reduces T_c , resulting in an effective single-band anisotropic superconductor in the dirty limit. This was first predicted for MgB_2 [19, 20] and later observed in

TABLE I: Superconducting gap parameters and relative DoS contributions from tunnelling (STS), heat capacity (HC) and AC susceptibility (ACS) data. Both gaps $\Delta_{1,2}$ are measured in meV. $\Gamma_{1,2} \leq 0.2 \text{ meV}$ for all STS fits.

		SnMo_6S_8		PbMo_6S_8	
technique		bulk		bulk	
T_c	ACS	$14.2 \pm 0.05 \text{ K}$		$14.9 \pm 0.15 \text{ K}$	
H_{c2}	HC	$42 \pm 1 \text{ T}$		$86 \pm 5 \text{ T}$	
γ	HC	$6.4 \pm 0.1 \text{ mJgat}^{-1}\text{K}^{-2}$		$6.7 \pm 0.1 \text{ mJgat}^{-1}\text{K}^{-2}$	
Δ_1	HC	3.06 ± 0.1		3.15 ± 0.1	
Δ_2	HC	0.86 ± 0.1		1.41 ± 0.1	
N_1	HC	$96 \pm 2\%$		$90 \pm 2\%$	
N_2	HC	$4 \pm 2\%$		$10 \pm 2\%$	
		Terrace	Step	Terrace	Step
Δ_1	STS	2.92 ± 0.1	2.95 ± 0.1	3.14 ± 0.15	3.06 ± 0.15
Δ_2	STS	–	1.05 ± 0.2	1.42 ± 0.2	1.36 ± 0.2
a_1	STS	0.85 ± 0.02	0.87 ± 0.02	0.85 ± 0.02	0.89 ± 0.02
a_2	STS	–	0.91 ± 0.1	0.92 ± 0.1	0.75 ± 0.1
N_1	STS	–	$62 \pm 4\%$	$90 \pm 4\%$	$66 \pm 4\%$
N_2	STS	–	$38 \pm 4\%$	$10 \pm 4\%$	$34 \pm 4\%$

irradiated samples [21]. However, due to extremely weak scattering between σ and π bands, the single band limit is never reached in MgB_2 . This may not be the case for CP: Fig. 2(c) displays a SnMo_6S_8 spectrum from a terrace after 3 months of measurements comprising numerous thermal and magnetic cycles. It is qualitatively similar to the results of [18] (shown in Fig. 2(f)), providing good evidence for low-energy states within the large gap, but does not display a distinct smaller gap. This is consistent with the presence of strong interband surface scattering. The ZBC is also rather high in both (c) and (f), which we attribute to a decrease in the superfluid density due to enhanced pair-breaking from inelastic scattering.

Upon increasing the temperature the large gap is gradually reduced and closes at the bulk T_c determined by ACS. No pseudogap is visible above T_c , confirming that superconductivity arises from a metallic ground state and hence justifying the use of a BCS model to fit the spectra. In Fig. 3 we have plotted the variation of the large gap Δ_1 with temperature for each compound, with the theoretical BCS weak-coupling s -wave curve for comparison. A small kink is visible within each curve (shaded

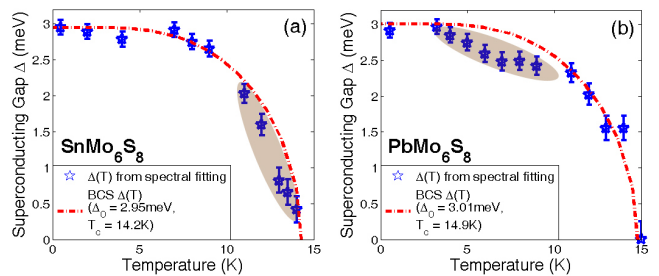


FIG. 3: Variation of $\Delta_1(T)$ in (a) SnMo_6S_8 and (b) PbMo_6S_8 . The gap was determined by fitting with a BCS single-band anisotropic s -wave model for simplicity and all spectra were acquired on a flat terrace.

areas). Similar features have been observed for the π -band (smaller) superconducting gap in MgB_2 and originate from interband scattering “stretching” the effective T_c of the weakly-coupled π band to the bulk T_c . We suggest that in CP a small contribution from a weakly-coupled band “stretches” the intrinsic T_c of a strongly-coupled band (which provides the majority of the DoS) to the measured bulk T_c . The position of the kink at higher energy and lower temperature in PbMo_6S_8 compared with SnMo_6S_8 is consistent with our observation that band 2 is more strongly-coupled in PbMo_6S_8 . We hypothesise that this may be the key to PbMo_6S_8 having a significantly higher H_{c2} than SnMo_6S_8 , although further experiments will be required for confirmation.

It is instructive to complement our STS measurements with bulk thermodynamic (HC) data, in order to conclusively rule out any spurious surface effects being responsible for Δ_2 . Figure 4 (a) and (b) display the electronic heat capacity C_{elec} in SnMo_6S_8 and PbMo_6S_8 : this is measured by subtracting the HC in an applied field $H = 28$ T from the zero-field data $C_{0\text{T}}$. To eliminate the effect of fluctuations above T_c in high field, we limit our data to $T > 1.15 T_c(28\text{T})$, where $T_c(28\text{T}) = 4.4$ K and 9.3 K in SnMo_6S_8 and PbMo_6S_8 respectively. In CP there is a large contribution to the lattice HC C_{latt} from a low-energy Einstein phonon due to vibrations of the cation between the Mo_6X_8 clusters: it is therefore not possible to calculate C_{latt} and hence extract C_{elec} using the conventional $\sum_{j=1}^n B_{2j+1} T^{2j+1}$ model. However, the Sommerfeld constant γ may still be calculated using entropy considerations (see Table I). We find that $\gamma/T_c = 0.45$ mJgat $^{-1}$ K $^{-3}$ in each compound, suggesting that T_c scales with the DoS at E_F . Using a two-band α -model [22] we have performed fits to C_{elec} and summarise our results in Table I. For both gaps, the values of $2\Delta/k_B T_c$ from our STS data agree perfectly with those from HC experiments. While it is not possible to quantitatively compare our STS-measured N_j (which also depends on the tunnelling matrix element) with the bulk N_j , the trends observed by each technique ($N_1 > N_2$) are qualitatively in agreement.

The final signature of 2-band superconductivity is provided by the low-temperature variation of $C_{\text{elec}}(H)$ in each material. In a single-band BCS s -wave superconductor $\gamma(H)$ should be linear. However, at $T = 0.35$ K we observe bends in $C_{\text{elec}}(H)$ at $H_x = 2.8 \pm 0.2$ T and 3.4 ± 1 T in SnMo_6S_8 and PbMo_6S_8 respectively, reminiscent of the low-field behaviour of MgB_2 . Extrapolating the high-field linear fits to the normal-state value for γ , we obtain $H_{c2} = 42 \pm 1$ T and 86 ± 5 T (although it should be noted that these may be slight overestimates due to vortex overlap effects at high field). We assume that H_x corresponds to the crossover between filling Δ_2 in band 2 followed by Δ_1 in band 1 and hence estimate $N_1 = 93 \pm 0.5$ %, $N_2 = 7 \pm 0.5$ % and $N_1 = 96 \pm 1$ %, $N_2 = 4 \pm 1$ % for SnMo_6S_8 and PbMo_6S_8 . These figures

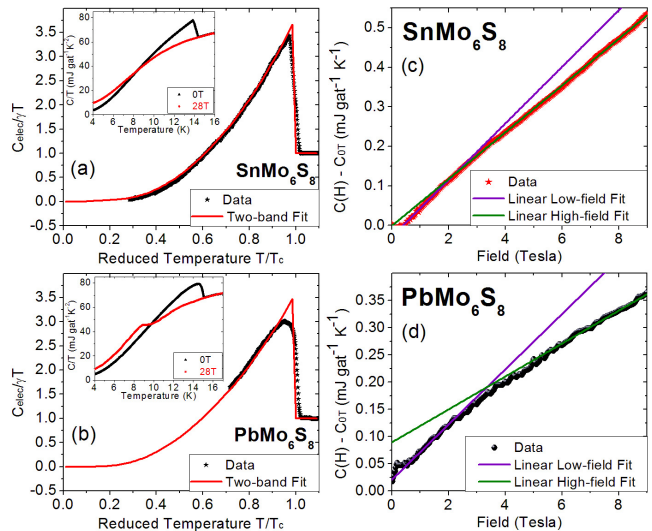


FIG. 4: (a),(b) $C_{\text{elec}}/\gamma T$ with two-band α -model fits [22]. Insets: C/T at 0 T and 28 T. (c),(d) Field-dependent contributions to C_{elec} at $T=0.35$ K with linear fits above and below the crossover field H_x (see text). The crossover in PbMo_6S_8 is rather broad compared to SnMo_6S_8 ; this is due to the lower homogeneity in the PbMo_6S_8 crystal as seen by increased transition widths in HC and ACS data.

are in good agreement with those in Table I.

Together, our spectroscopic and thermodynamic data provide compelling evidence for a multi-band order parameter in CP superconductors. In both SnMo_6S_8 and PbMo_6S_8 , a strongly-coupled quasi-isotropic band (contributing the majority of the DoS at E_F) coexists with a highly anisotropic weakly-coupled minority band. Looking ahead, we postulate that understanding and manipulating the interplay between two or more such bands may hold the secret to realising high values for H_{c2} in future superconducting materials.

- [1] Ø. Fischer, Appl. Phys. **16**, 1 (1978).
- [2] R. Chevrel, M. Sergent, and J. Prigent, J. Solid State Chem. **3**, 515 (1971).
- [3] M. Decroux and Ø. Fischer, *Topics in Current Physics: Superconductivity in Ternary Compounds II* (Springer-Verlag Berlin Heidelberg New York, 1982), pp. 57–87.
- [4] H. Suhl, B. Matthias, and L. Walker, Phys. Rev. Lett. **3**, 552 (1959).
- [5] L. Shen, N. Senozan, and N. Phillips, Phys. Rev. Lett. **14**, 1025 (1965).
- [6] G. Binnig, A. Baratoff, H.E. Hoenig, and J.G. Bednorz, Phys. Rev. Lett. **45**, 1352 (1980).
- [7] J. Nagamatsu, N. Nakagawa, T. Muranaka, Y. Zenitani, and J. Akimitsu, Nature **410**, 63 (2001).
- [8] M.R. Eskildsen, N. Jenkins, G. Levy, M. Kugler, Ø. Fischer, J. Jun, S. M. Kazakov, and J. Karpinski, Phys. Rev. B **68**, 100508 (2003).
- [9] F. Bouquet, Y. Wang, I. Sheikin, T. Plackowski,

- A. Junod, S. Lee, and S. Tajima, *Phys. Rev. Lett.* **89**, 257001 (2002).
- [10] B. Bergk, V. Petzold, H. Rosner, S.-L. Drechsler, M. Bartkowiak, O. Ignatchik, A.D. Bianchi, I. Sheikin, P.C. Canfield, and J. Wosnitza, *Phys. Rev. Lett.* **100**, 257004 (2008).
- [11] S. Kuroiwa, Y. Saura, J. Akimitsu, M. Hiraishi, M. Miyazaki, K.H. Satoh, S. Takeshita, and R. Kadono, *Phys. Rev. Lett.* **100**, 097002 (2008).
- [12] R.W. Hill, S. Li, M.B. Maple, and L. Taillefer, *Phys. Rev. Lett.* **101**, 237005 (2008).
- [13] F. Hunte, J. Jaroszynski, A. Gurevich, D. Larbalestier, R. Jin, A. Sefat, M. McGuire, B. Sales, D. Christen, and D. Mandrus, *Nature* **453**, 903 (2008).
- [14] O.K. Andersen, W. Klose, and H. Nohl, *Phys. Rev. B* **17**, 1209 (1978).
- [15] Previous experiments on PbMo_6S_8 in the 1970s suggested $H_{c2} \sim 55\text{-}60$ T. However, recent data from oxygen-free crystals (including our specific heat-derived value in Table I) reveal a significantly higher H_{c2} of at least 80 T.
- [16] R. Lortz, Y. Wang, A. Demuer, P.H.M. Böttger, B. Bergk, G. Zwicknagl, Y. Nakazawa, and J. Wosnitza, *Phys. Rev. Lett.* **99**, 187002 (2007).
- [17] W.L. McMillan, *Phys. Rev.* **175**, 537 (1968).
- [18] C. Dubois, A. Petrović, G. Santi, C. Berthod, A.A. Manuel, M. Decroux, Ø. Fischer, M. Potel, and R. Chevrel, *Phys. Rev. B* **75**, 104501 (2007).
- [19] A.Y. Liu, I.I. Mazin, and J. Kortus, *Phys. Rev. Lett.* **87**, 087005 (2001).
- [20] I.I. Mazin, O.K. Andersen, O. Jepsen, O.V. Dolgov, J. Kortus, A.A. Golubov, A.B. Kuz'menko, and D. van der Marel, *Phys. Rev. Lett.* **89**, 107002 (2002).
- [21] Y. Wang, F. Bouquet, I. Sheikin, P. Toulemonde, B. Revaz, M. Eisterer, H. Weber, J. Hinderer, and A. Junod, *J. Phys.: Condens. Matter* **15**, 883 (2003).
- [22] H. Padamsee, J. Neighbor, and C. Shiffman, *J. Low Temp. Phys.* **12**, 387 (1973).